NATO: Development of Biosensors using Carbon Nanotubes

S. Bellucci (Project Director), R. Baldini (Tecn.), S.Bistarelli (Dott.), A. Cataldo (Dott..), F. Micciulla (Ass. Ric.)
External collaborating Institutions:
- Yerevan State Univ., Armenia

We direct the project Development of Biosensors using Carbon Nanotubes within the NATO Emerging Security Challenges Division, Science for Peace and Security Programme. The project has a duration of 42 months and started its activities on 1st October 2013. The consortium binds together a University and a Research Organization.

Abstract & Current Status

The main direction of the antiterrorist defence is the prevention and/or the early exposure of terroristic attacks. In case of using the biological warfare such as living agents or toxins DNA – biosensors yield one of the most effective tools for early diagnostics. The main goal of the Project is creation of a reliable, sensitive, selective and noise protected prototype of a DNA biosensor. Currently we have: quantitative understanding of the mechanisms of hybridization in the bulk and on the surface; the main ways to improve DNA sensors sensitivity and selectivity; the electric scheme of the DNA – sensor prototype.

Project Goals

The main direction of the antiterrorist is the prevention and/or the early exposure of terroristic attacks. In case of using the biological warfare such as living agents or toxins DNA – biosensors yield one of the most effective tools for early diagnostics. The main objectives of the project are:

I) To create a prototype of one of the technologically state-of-the-art and most effective electrochemical DNA – biosensors.

ii) To investigate and to compare thermodynamics and kinetics of DNA and RNA hybridization both in the bulk and when immobilized on the surface of a substrate, e.g. an electrode

iii) To synthesize polymer – CNT nanocomposites as suitable candidates for biosensor electrodes.

iv) To investigate sensitivity, selectivity and “noise immunity” of DNA-sensors, using a polymer – CNT substrate and agents for the registration of hybridization

v) To develop measuring methods for the registration of the changes in biosensors properties stimulated by DNA hybridization or other processes

Summary of Accomplishments

- We have prepared in laboratory graphene nanoplates (GNPs) with exfoliation assisted by microwave. GNPs were obtained in laboratory by microwave irradiation. Polymer – CNT substrates and GNP composites are synthesized. The samples were analyzed with At-IR spectroscopy and Scanning Electron Microscopy.
- The key factors for the stability of double – stranded Nucleic Acids in presence of metal – containing porphyrins and bivalent cations are estimated using Circular Dichroisme.

- The model, describing kinetics of the single – stranded RNA folding and hybridization is developed.
- The model, describing equilibrium isotherm of hybridization of single – stranded nucleic acids immobilized on surface in presence of ligands is developed.
- The way to improve mechanical and electric features of the polymer substrate, armed by CNTs is proposed on the basis of crystallization, promoted by CNTs as a centres of nucleation.
- The approach to control the CNTs' alignment in the polymer matrix is proposed.
- The absorption spectra of the ssDNA dissolved in solution is measured both with and without polymer-CNT substrate.
- The interaction between functionalized CNTs and miRNA is addressed.
- The electric scheme of the DNA – biosensor prototype is developed
- The controlling software for the DNA – biosensor prototype is developed
- The simulation of the force unzipping of the dsDNA is made
- The nanocomposite modified screen printed electrodes are produced
- The electrochemical characterization of nanocomposite modified screen printed electrodes are made
- The impulse acoustic microscopy characterization of the nanocarbon cluster architecture in the composite to modify screen printed electrodes is made
- The Raman characterization of nanocomposite modified screen printed electrodes is made

Accomplishments

I. Stability of DNA – ligand complexes:

The higher affinity of the certain porphyrins to the double – stranded regions of Nucleic Acids (NA) in comparison to single – stranded is important for the hybridization thermodynamics and kinetics. UV-VIS spectrophotometry and circular dichroism (CD) methods were applied to study the binding of the different kinds of porphyrins, including TOEPyP4), CuTMPyP4 etc. with double – stranded DNA. The binding constants K_b

and stoichiometry *n* were determined from absorbance spectra. The free energy, enthalpy and entropy of binding also were calculated using the values of $K_{b.}$.

Materials and methods

Ultra-pure DNA from calf thymus (protein < 0.1%, RNA < 0.2%, M. w. > 30 MDa; GC = 42%) was a kind gift from prof. D.Yu. Lando at the Institute of Bioorganic Chemistry (Minsk Belarus). Porphyrins were synthesized in the Department of Pharmacological Chemistry, Yerevan State Medical University. All spectroscopic measurements were performed in 0.1 BPSE buffer (1BPSE = 6 mM Na2HPO4 + 2 mM NaH2PO4 + 185 mM NaCl+ 1 mM EDTA), pH 7, 0. The melting experiments were performed in 10 − 3 M NaCl solution, as in 0.1 BPSE buffer (ionic strength μ = 0.02) this complexes are much stabilized and experimentally impossible to finish melting process. The pH of the solutions used throughout the experiments were kept constant at 7.0 ± 0.1. A stock solution of DNA was prepared in 10 − 3 M NaCl solution at pH 7,0. An extinction coefficient ε260 = 1.31 × 104 M−1 cm−1 was applied to determine the concentration of DNA in base pairs. Porphyrin concentrations and extinction coefficient of CuTButPyP4 and CoTButPyP4 porphyrins were determined by spectrophotometric method and are respectively equal ε427 = 1.08 × 105 M−1 cm−1 and ε437 = 0.74 × 105 M−1 cm−1. The porphyrin solutions were prepared before each experiment and were kept in the dark. Visible absorption spectra of the porphyrins in the Soret region in the absence and presence of the DNA duplexes were collected at 20 °C using Perkin Elmer Lambda 800 UV/VIS spectrophotometer. CD spectra were recorded at 20 °C on Dichrograph Roussel Jouan-II. Melting curves were recorded on Perkin Elmer Lambda 800 UV/VIS spectrophotometer with heating rate 0.5–1 °C/min.

Main results

The characteristics of porphyrin complexation with the DNA were investigated using a special technique of circular dichroism (CD), by means of which not only conformational changes in the DNA molecule, but also the preferred type of binding of the porphyrin with DNA and polynucleotides can be exactly determined. CD spectra of DNA duplexes with and without porphyrins were recorded by the Olis DSM spectrophotometer in quartz cuvettes (Perkin Elmer), at 25° C. CD titration was measured by adding multiple aliquots of porphyrin solution to a known amount of DNA solution. We use CD spectra (Fig. A.1.3) to identify the binding mode for DNA duplexes in the presence of porphyrins. Fig. A.1.3 shows the circular dichroism

spectra for B- and A-DNA at different relative concentrations (r), where r = C_{Porph}/C_{DNA}. It is known that intercalating molecules are well placed in the minor grooves of the DNA double helix and have a negative CD spectrum with relatively large ellipticity. Fig. A.1.3 presents the CD spectra of B-DNA with TOEPyP4 porphyrin (panel A) at 25°C.

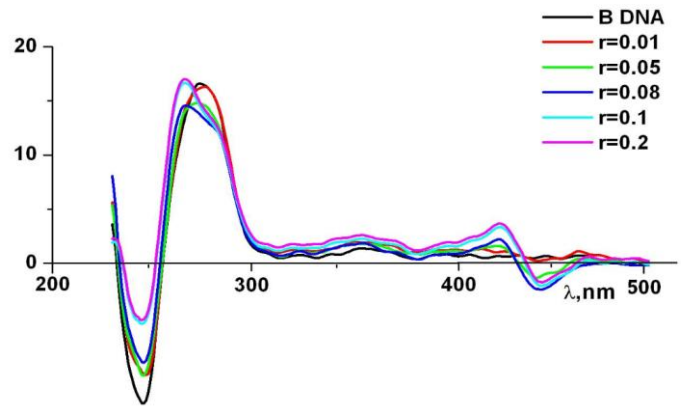

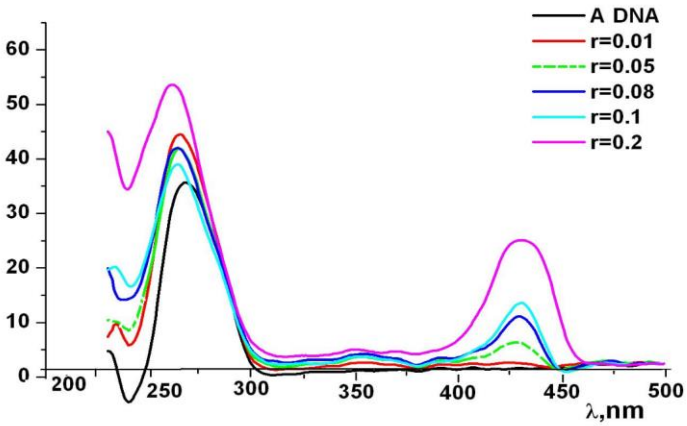

Fig. 1. ICD-spectra of complexes of B-DNA with TOEPyP4 and of A-DNA with TOEPyP4

A strong conservative CD spectrum in the Soret region of the DNA-TOEPyP4 complex is due to the existence of two types of complexes: intercalation and outside binding. As shown from Fig. 1 (panel B), the addition of porphyrin concentration in A DNA leads to the appearance of positive ICD spectrum. Fig. 1 shows that TOEPyP4 porphyrin tended to intercalate into the B-DNA, rather than A-DNA, but in case of high values of relative concentration *r* the external binding takes place. As it can be seen from Fig. 1 (panel B) TOEPyP4 interacts with A DNA only through external groove binding that is conditioned by A DNA conformation.

To determine the binding modes of the studied porphyrins, the CD spectra of porphyrin/DNA complexes were measured for the various concentrations of porphyrins at the fixed concentration of DNA in solution. DNAs with various values of GC – content were addressed. The melting parameters of DNA in presence of porphyrins at ionic strength μ = 0.001 are summarized in Table 1.

r=[P]/[DNA]	CuButPyP4/DNA		CoButPyP4/DNA	
	T_m	ΔT	T_m	ΔT
0	54.6	13.2	54.6	13.2
0.001	53.8	13.01	54.53	13.38
0.01	55.9	13.0	56.06	14.5
0.03	59.6	15.34	58.86	17.58
0.05	70.4	16.85	61.68	18.85
0.1	62.65	12.65	68.35	21.9

The investigation of the UV and CD spectra of DNA – porphyrin complexes also clearly show that:

- **Binding mode of DNA – porphyrins binding depends on the form of DNA double helix (A-form or B-form)**
- **The binding mode of porphyrins with DNA also depends on the relative concentration of porphyrin and DNA, the nature of DNA and porphyrins (the central metal, type of the peripheral substituents and etc.).**

- **Porphyrins, depending on their structure, and the presence of the coordinated metal including possible axial ligands, display different preferences not only for binding modes, but also for different DNA sequences.**

II. DNA – sensor substrate development

Preparation of the polymer - CNT and GNP composites and microscopic characterization, synthesis and oxidation of graphene nanoplates

The composite with CNT was prepared in this way: to start with, the CNTs were weighed and required wt% of the CNT is mixed in Isopropylic acid and ultrasonicated for 30 min. Then this solution is mixed with known quantity (weight) of resin and heated in an oven for 2 hr at 80°C. The alcohol evaporates off and the resin with CNT is again sonicated for 15 min. Immediately after this the hardener is mixed and the mixture is applied on the surface of the electrical circuit and allowed to set. The wide spectrum of polymer – CNT composites was prepared for the subsequent measurements:

- epoxy resins, containing 0.25, 0.5, 0.75 and 1.0 % of the MWCNTs 20 – 30 and 30 – 50
- epoxy resins, containing 0.25 and 0.5 % of the COOH functionalized MWCNTs
- pure epoxy resins

In order to add functional groups on the surface of CNT, we have carried out treatment of oxidation on samples of CNT (outer diameter=8-15 nm). Nitric acid solution (65% vol) and Piranha mixture (ratio sulfuric acid 96%/hydrogen peroxide 30% in volume 7:3 respectively) have been used as oxidant media. Furthermore, both media was used in two different experimental condition: reflux condition and sonication condition:

- Under reflux condition, we have put 0.15 g of CNT in a round bottom flask with 25mL of media (HNO_3 or Piranha mixture). Mixture was heated to obtain reflux condition and maintain it for 4 h.
- Under sonication condition, we have put 0.15 g CNT in a becker with 25 mL of media (HNO_3 or Piranha mixture) and have put in a ultrasonic bath. We have maintained dispersion in sonication for 4 h.

After oxidant treatment, we have filtered and washed with distillated water. We have dried samples in air at room temperature. The samples were analysed

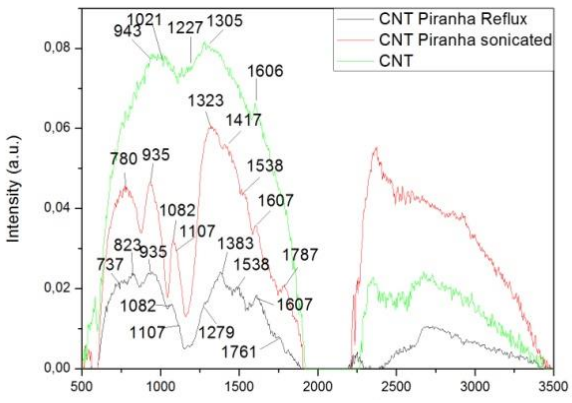

Fig. 2. Oxidazed CNT with HNO3 and Piranha

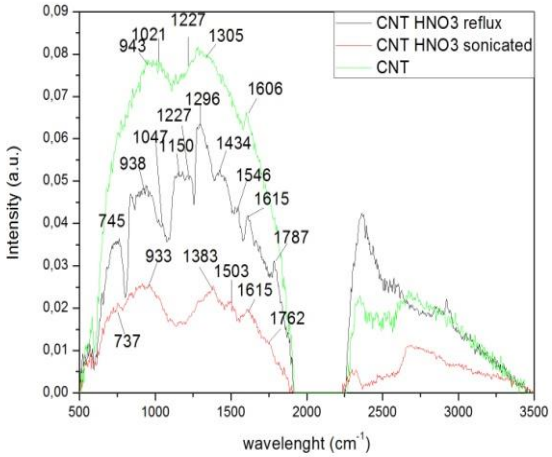

using At-IR spectroscopy.

In the Fig. 2, we observe an evolution from pristine CNT spectrum to treated CNT: in particular, peaks at ~1500, 1600 and 1700 cm^{-1}, relative to oxidrilic and carbonyl group, appear in treated CNT. Peak at ~3300cm^{-1} doesn't appear, so we can conclude that we add in CNT hydro and carbonyl groups. Different approaches of oxidation lead to the same result. All founded peaks are listed in Table 1 presented below:

Table 2. IR Bands Observed in the Raw and Chemically Processed CNT

Pristine CNT	CNT HNO3 reflux	CNT HNO3 sonicated	CNT piranha sonicated	CNT piranha reflux
	740	730	775	775
	938	940	935	935
	1047		980	980
1100	1100		1080	1080
1200	1200		1100	1100
1300	1290		1325	1380

	1400	1380	1408	1408
	1544	1530	1530	1530
1600	1620	1620	1600	1600
	1780	1760?	1790	1790

We also prepared graphene nanoplates (GNPs) with exfoliation assisted by microwave. GNPs were obtained in laboratory by microwave irradiation. Expandable Graphite (EG) Asbury® was used as carbon source: EG was put in home microwave oven, with a power of 800W, inside a ceramic melting pot. About ten seconds of irradiation are enough to produce expansion of EG and formation of worm-like particles: the process of expansion was carried out by thermal shock due to microwave irradiation that warms EG and vaporize molecules present inside EG planes. Furthermore, thermal shock was also caused by sparks that occur during the process: vaporized molecules change dielectric constant of atmosphere and electric arc occurs. GNPs particles were obtained with mild sonication in ultrasonic bath for ten minutes. Particles were from 4 to 9nm thick (4-11 layers) and from 2 to 10μm large. About nanocomposite, we have decided to prepare epoxy nanocomposites adding GNPs, too. GNPs were weighed and required wt% of the GNP is mixed in Isopropylic acid and ultrasonicated for 30 min. Then this solution is mixed with known quantity (weight) of resin and heated in an oven for 2 hr at 80°C. The alcohol evaporates off and the resin with GNP is again sonicated for 15 min. Immediately after this the hardener is mixed and the mixture is applied on the surface of the electrical circuit and allowed to set. The wide spectrum of polymer – GNP composites was prepared for the subsequent measurements.

In order to add functional groups on the surface of GNPs, we have carried out oxidation treatment. Nitric acid solution (65% vol) and Piranha mixture (ratio sulfuric acid 96%/hydrogen peroxide 30% in volume 7:3 respectively) have been used as oxidant media. Furthermore, both media was used in two different experimental condition: reflux condition and sonication condition:

- In reflux condition, we have put 0.15 g of GNP in a round bottom flask with 25mL of media (HNO3 or Piranha mixture). Mixture was heated to obtain reflux condition and maintain it for 4 h.

- In sonication condition, we have put 0.15 g of GNP in a becker with 25 mL of media (HNO3 or Piranha mixture) and have put in a ultrasonic bath. We have maintained dispersion in sonication for 4 h.

After oxidant treatment, we have filtered and washed with distillated water. We have dried samples in air at room temperature. The samples were analyzed with At-IR spectroscopy. Results and discussion are presented in the Fig.3.

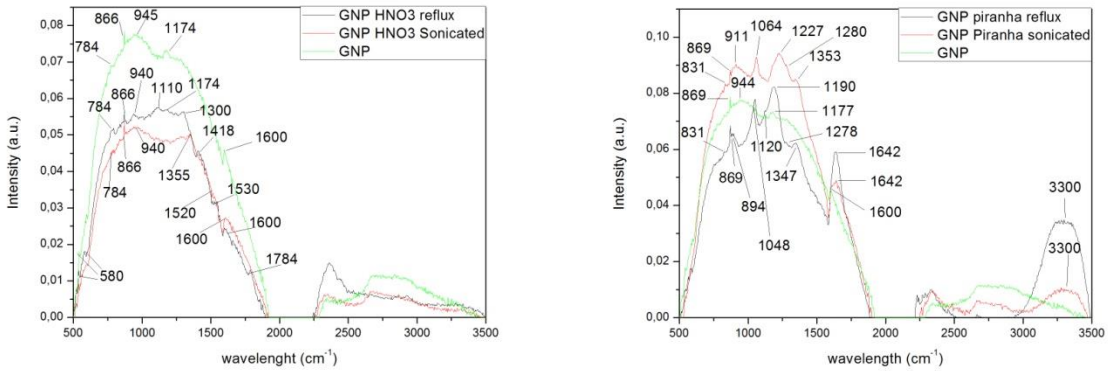

Fig. 3. Oxidized GNP with HNO3 and Piranha

From the Fig. 3, we observe an evolution from pristine GNP spectrum to treated GNP: in particular, peaks at ~1500, 1600 and 1700 cm-1, relative to oxidrilic and carbonyl group, appear in treated GNP. Furthermore, peak at ~3300cm-1 appears in samples treated with piranha mixture as media. This is an important and interesting results that we would confirm with further analysis. If this results will be confirmed, it means that we can add different functional groups varying experimental conditions, from hydro and carbonyl groups to carboxylic groups.

All found peaks are listed in Table 3 below:

Table 3. IR Bands Observed in the Raw and Chemically Processed GNP

GNP	GNP HNO3 reflux	GNP HNO3 Sonicated	GNP piranha sonicated	GNP piranha reflux

866	866	866	866	866
940	940	940	834	834
			918	900
	1110		1060	1048
1170	1170		1180	1120
	1300	1350	1220	1190
			1280	1278
	1420		1350	1350
	1530	1520		
1600	1600	1600	1640	1640
	1790			
			3300	3300

Surface characterization of CNT – and GNP – containing composites

The polymer - CNT composites, synthesized in the group of LNF, INFN were investigated by one of the members of the group from the Yerevan State University at the Advanced Technology and Nanoscience National Lab (Trieste, Elettra) with the Scanning Electron Microscope (SEM) Zeiss Supra-40 and VEGAII scanning electron microscopy (see Figs. 4 – 6). According to performed measurements, the characteristic scale of roughness, which is maximal at the place we are cutting the sample. From another sides the surface is more smooth, with the scale or roughness about 1-2 micro meters. The roughness of the surface is a substantial obstacle for the single – stranded nucleic acids probes immobilization.

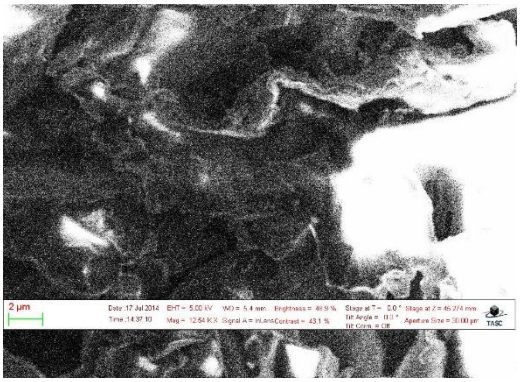

Fig. 4. The epoxy resins containing, 0.25% MWCNT by weight.

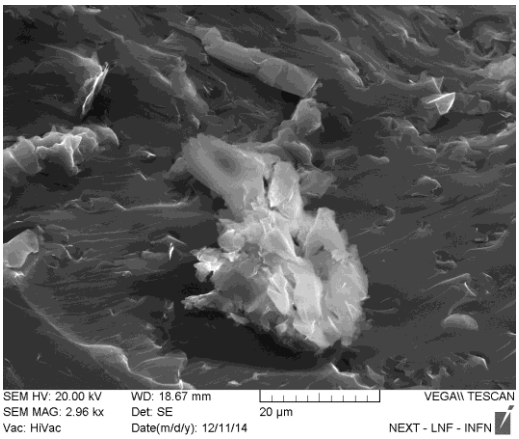

Fig. 5. Scanning electron micrographs of nanocomposite Epoxy/GNP.

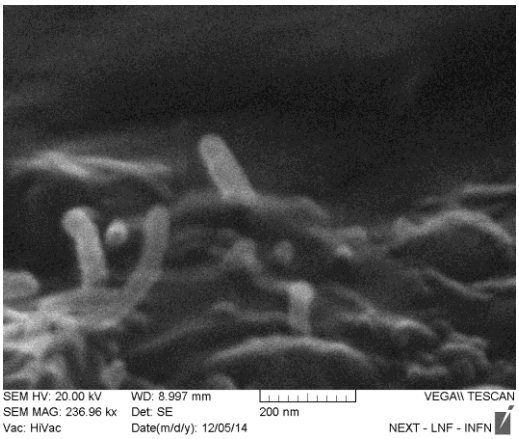

Fig. 1. Scanning electron micrographs of nanocomposite Epoxy/CNT.

Functionalization of GNPs with porphyrin.

To increase affinity of porphyrins to the DNA – sensor substrate we implement GNP functionalization with Prato's reaction in collaboration with Prof. P. Tagliatesta (University of Roma Tor Vergata).

We use an aldehydic substrate containing both a porphyrin and a ferrocene, linked by a triple bond each one.

The reaction develop as scheme reaction presented in the Fig. 7.

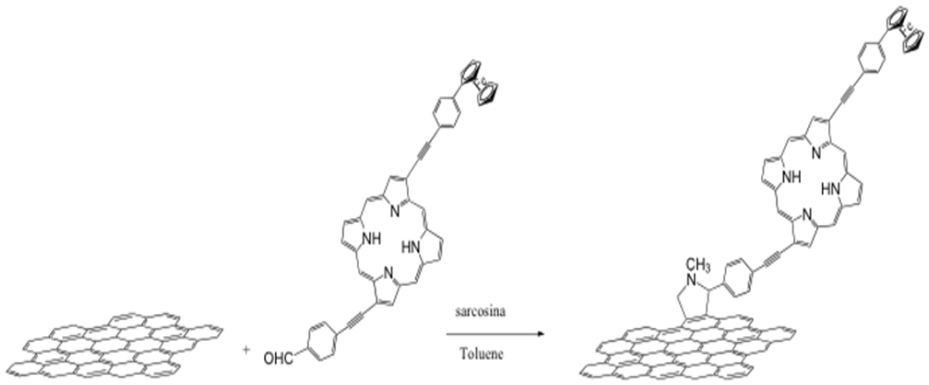

Fig. 7. Prato's reaction on GNP as substrate

After reaction, we observe functionalized GNP by SEM to check transformation on morphology of substrate.

The following figures represent a sample of pristine GNP and functionalized GNP:

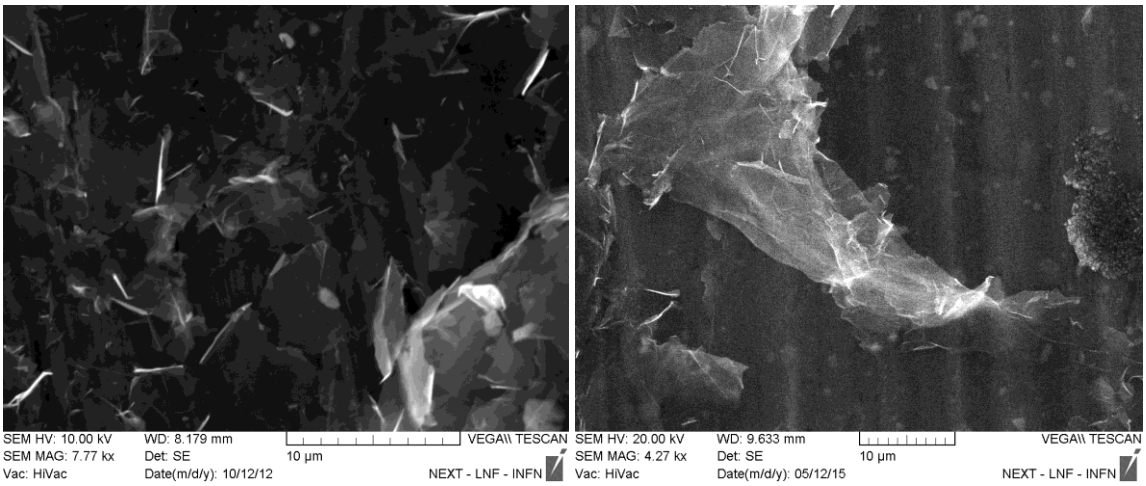

Fig. 2. (Left pane) Micrograph of pristine GNP. (Right pane) Micrograph of functionalized GNP.

To confirm the functionalization, we characterized the material with Raman spectroscopy in collaboration with Dr. V. Mussi (CNR-ISC). The comparison between the spectra of pristine and functionalized GNP reveals that functionalization occurs. Indeed, new peaks appear in the spectrum of functionalized GNP, attributable to presence of porphyrin/ferrocene. The shift of G and G' band of graphene at higher wavenumber confirms that functionalization occurs.

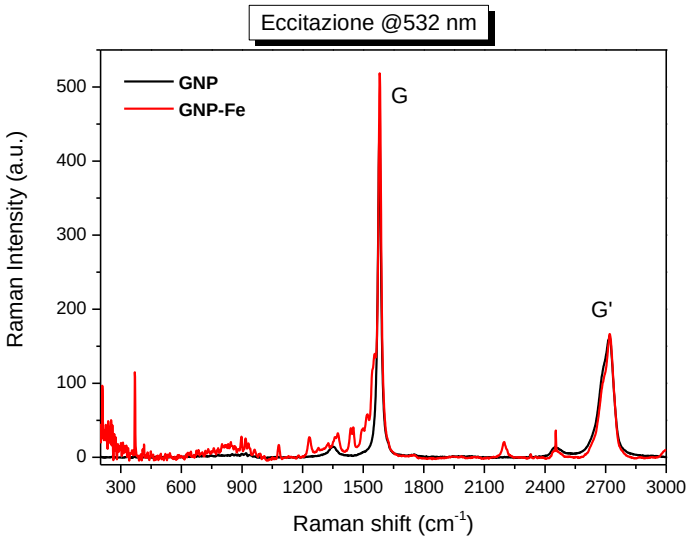

Fig. 9. Raman spectrum of pristine and functionalized GNP

Enlarge spectra is presented in the Fig. 10.

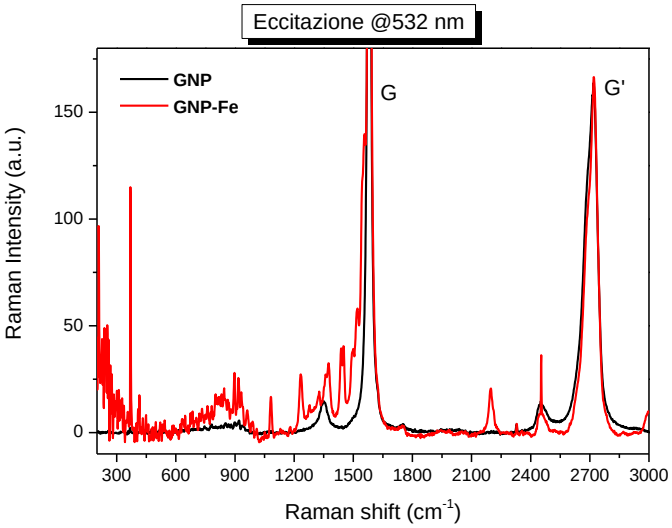

Fig. 3 Raman spectrum of pristine and functionalized GNP zoom in

Electrochemical analysis of CNT – and GNP – containing composites

We have investigated the electrochemical behavior of pure epoxy resin and epoxy resin loaded with CNT and GNP. This study has been performed EIS and CV characterization by using PalmSens3 instrument.

Pure Epoxy resin

The first step consists in studying the electrochemical behavior of pure epoxy resin performing a CV. We have chosen as experimental setup: a solution 1 mM of K3[Fe(CN)6], a voltage range of -0.1/0.6 V, 100 mV/s scan rate, Ag/AgCl as reference electrode. As we can see in the following graphic, the redox process for the species Fe2+/Fe3+ in solution does not occur at the resin interface.

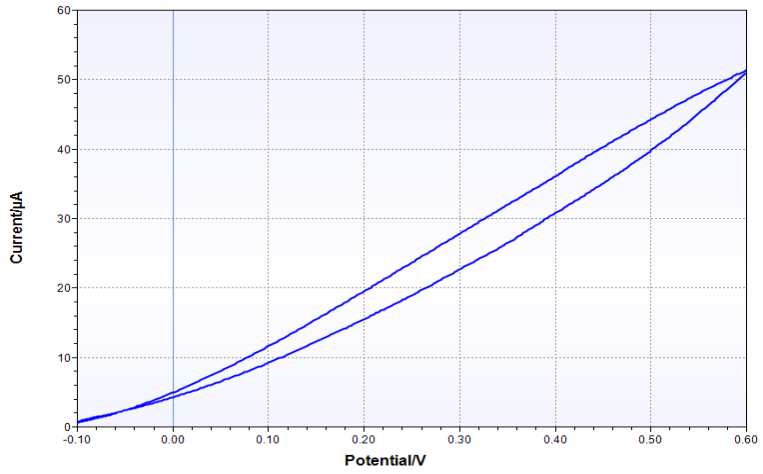

Fig. 11. CV epoxy resin

It is possible to go deep about epoxy-resin interface behavior performing an EIS in the same solution mentioned before. We have scanned the frequencies range 10000/5 Hz. Nyquist plot confirms the CV result. This is a preliminary and qualitative study, we are working to find a fitting circuit to evaluate the RCT.

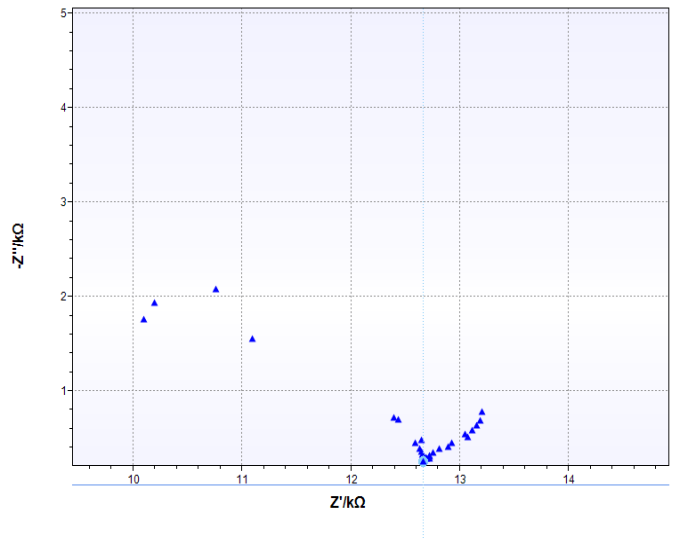

Fig. 12. Nyquist plot epoxy resin

GNP composite

We tried to improve the epoxy resin electrochemical behavior by adding GNP realizing a nanocomposite. We have used the same experimental setup to performing CV characterization. We found performing a CV is that the electrochemical properties do not improve at all. Nevertheless, the EIS performance shows a reduced RCT, as we can see in the figure 18, which suggests us an increasing of electrical properties compared with pure epoxy resin. We are working to find a fitting circuit to evaluate the RCT. The next investigation will be performed by adding CNTs to resin and investigate how they improve electrochemical composite behaviour. Furthermore, we will investigate any functionalization of nanocomposite surface to improve electrochemical properties.

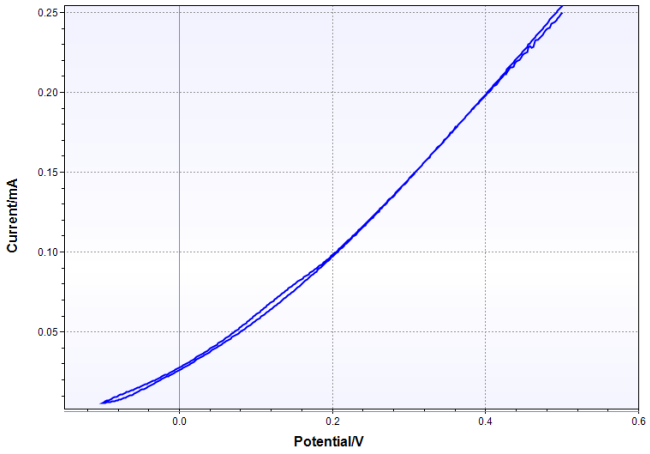

Fig. 13. CV GNP nanocomposite 0.75%w/w

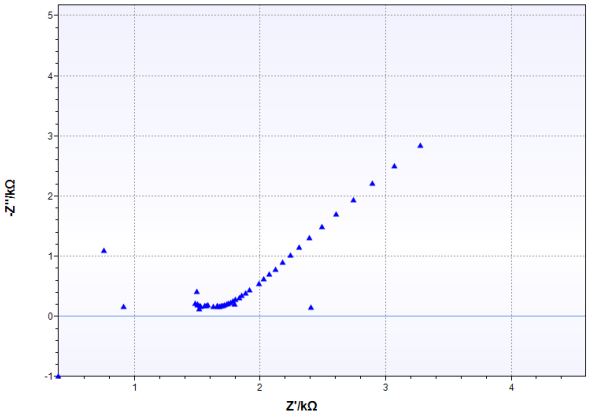

Fig. 14. Nyqist plot GNP composite 0.75%w/w

Preparation of nanocomposite materials with Thinky planetary mixer

To improve the homogeneity of nanocomposite we performed experiments using Thinky planetary mixer. We have worked in vacuum (3mbar) and changed mixing velocity. To test the new instrument at critical condition, we have prepared a nanocomposite loaded with 10%w/w of MWCNT 30-50 nm.

After preparation, nanocomposite appears uniform and without bubble, as shown by picture reported below

Fig. 15. Nanocomposite Epoxy/CNT 10% w/w

We characterized sample with SEM and we observed the two side: the one attached to beaker and the one to the air.

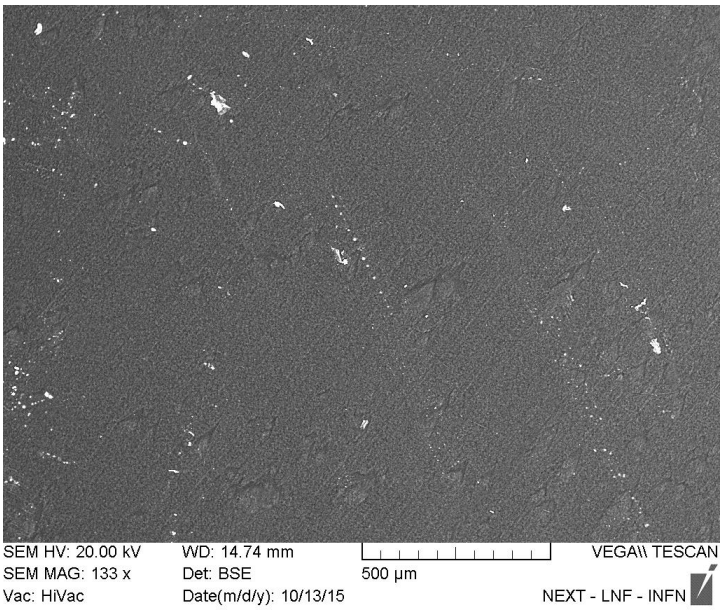

Fig. 16. Micrograph of Nanocomposite Epoxy/CNT 10% w/w on air side

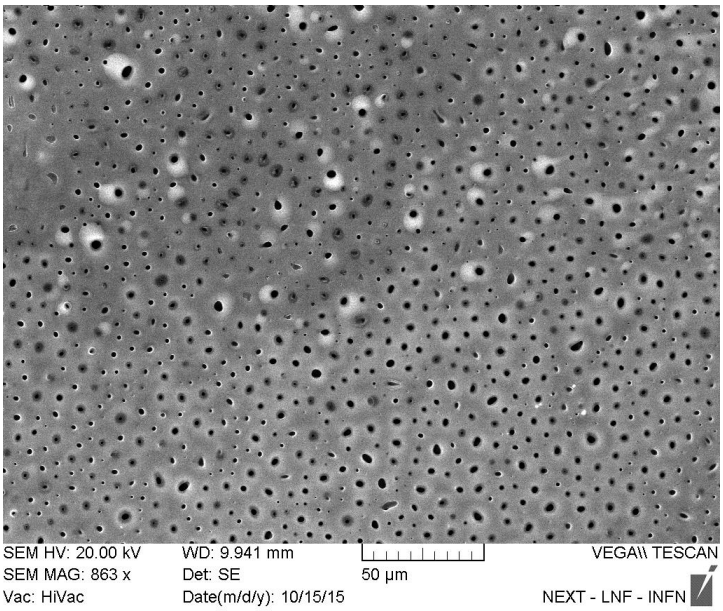

Fig. 17. Micrograph of Nanocomposite Epoxy/CNT 10% w/w on beaker side

We can see from these pictures that:

- **matrix has not bubbles of air inside;**
- **MWCNT are well dispersed in matrix, although some aggregates;**
- **matrix from beaker side copy the structure of beaker.**

The obtained results are promising to improve homogeneity of nanocomposites.

Preparation of soluble multifunctional carbon nanotubes

We used pristine and carboxy (COOH) functionalized carbon nanotubes (CNTs), for preparing functional nanomaterials coated with polyethylenimine (PEI) and polyamidoamine (PAMAM) polymers, followed by conjugation of miR-503 oligonucleotides to address the interaction between nucleic acids and CNTs. Simple physicochemical adsorption allowed us to coat CNTs, whereas polymer-conjugated CNTs have been obtained by amide bonds formation by taking advantage of COOH functionalities. Different functionalized CNTs display different solubility and toxicity properties, as a function of the polymer molecular weight. We evaluated the properties of these functional nanomaterials (i.e. DNA binding ability, toxicity, transfection efficiency) by specific in vitro assays (i.e., gel electrophoresis, cell cultures and fluorescence microscopy) on human primary endothelial cells.

Preparation of nanocomposite modified screen printed electrodes

In order to test the electrochemical properties of nanocomposites, we modified Screen-printed electrodes based on carbon with nanocomposites, varying type and amount of fillers. The screen printed system, provided by Dropsens, is made by a working (4 mm diameter) and counter electrodes made of carbon. The Reference electrode and electric contacts made of silver, shown in the Fig.18.

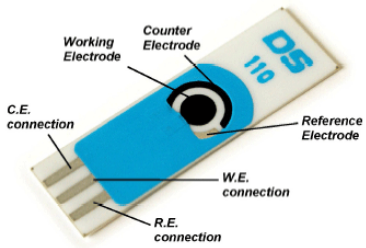

Fig. 18. The unmodified screen printed electrode

The working electrode is the sensing part of the screen printed system. In order to test the electrochemical behavior of nanocomposite, we modified the Screen-printed electrodes dropping on the working electrode the epoxy nanocomposite, varying type of fillers and their concentration. To prepare nanocomposites, we used the planetary mixer, Thinky, bought by NATO funding.

We used three different types of carbon nanofiller, with different morphological structures, i.e. one dimensional (CNTs), as well as two dimensional ones (GNPs), prepared according to methods developed in our laboratory:

- Multi-Walled carbon nanotube, diameter 8-15 nm (we will call them CNT);
- Multi-Walled carbon nanotube, diameter 10-20 nm, functionalized by amino groups –NH2 (we will call CNT-NH2);
- Graphene nanoplatelets obtained in laboratory by microwave exfoliation [2-8] (we will call them GNP).

For each filler, we prepared nanocomposite at 0.25, 1, 2 and 10%. In the range 0.25-2%, we dispersed filler directly in epoxy resin using an ultrasonic tip for 5 min. After the ultrasonic treatment, we put the mixture in Thinky and run the program to eliminate unwanted bubbles, possibly introduced during sonication, and mix filler particles with resin. Finally, we added curing agent to cross-link the resin. Furthermore, before cross-link happened, we deposited a droplet of nanocomposite with a stick, trying to cover completely the surface of working electrode.

In the case of loading at 10% in weight of filler, the amount of the latter is so high that ultrasonic tip was not able to disperse the nanoparticles. Therefore, we modified the procedure and used just Thinky mixer: the high amount of filler, increases dramatically the viscosity of the resin. In these conditions, the Thinky planetary movement worked efficiently and dispersed nanoparticles in the resin. Also in this case, we deposited a droplet of nanocomposite with a stick, trying to cover completely the surface of working electrode.

The so-modified screen-printed electrodes, shown in the Fig. 18, were tested with galvanostat/potentiostat Palmsens also bought with the NATO funding.

Electrochemical characterization of nanocomposite modified screen printed electrodes

The electrochemical behavior of screen printed electrode modified with nanocomposite was investigated by galvanostat/potentiostat Palmsens. Firstly, we studied the electrochemical behavior by cyclic voltammetry, CV. The experimental setup was: 1 mM solution of K3[Fe(CN)6], voltage range of -0.1/0.6 V, 100 mV/s scan rate. In comparison with electrochemical behaviour, exhibit by massive piece of nanocomposite, the nanocomposite modified screen-printed electrodes have a good signal. The results are reported in the following graphs:

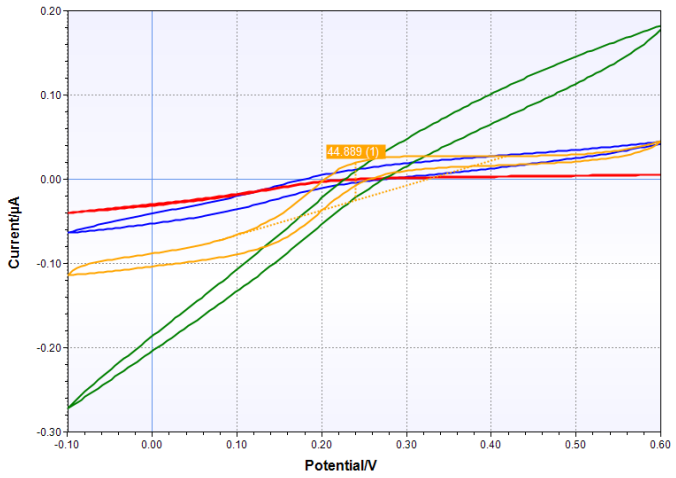

Fig. 19. CV of epoxy resin (yellow curve), and nanocomposite Epoxy-CNT 0.25, 1 and 2% (red, blue and green curve, respectively)

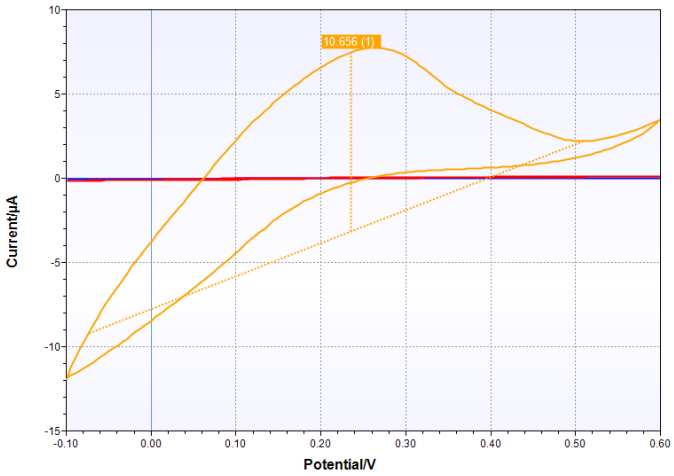

Fig. 20. CV of nanocomposite Epoxy-CNT-NH2 0.25, 1 and 2% (blue, red and yellow curve, respectively)

The obtained results are promising to obtain a major sensibility of nanocomposite modified electrodes.

In the Table 4 are summarised results of CV for unmodified screen printed electrodes and nanocomposite modified ones.

Table 4. Summary of data of CV for all electrodes analyzed

	Cathodic Potential (V)	Height of Cathodic Peak (µA)	Area of Cathodic Peak (µA·V)	Anodic Potential (V)	Height of Anodic Peak (µA)	Area of Anodic Peak (µA·V)
Unmodified electrodes	0,195	9,798	2,290	0,069	-6,888	1,012
CNT 0,25%	0,144	0,264	0,035	0,124	-0,204	0,020
CNT 1%	0,144	0,313	0,074	N.A.	N.A.	N.A.
CNT 2%	0,151	0,070	0,009	0,134	-0,049	0,005
CNT 10%	0,144	0,257	0,037	0,088	-0,177	0,020
CNT-NH2 0,25%	0,144	0,181	0,028	0,093	-0,118	0,013
CNT-NH2 10% n.c.	0,103	11,583	2,254	0,051	-9,605	1,095

CNT-NH2 10%	0,167	17,423	4,871	0,063	-9,580	1,337
GNP 10% n.c.	0,112	12,630	2,119	0,068	-9,695	1,200
GNP 10%	0,142	18,720	4,529	0,051	-10,745	1,567

Impulse acoustic microscopy characterization of the nanocarbon cluster architecture in the composite to modify screen printed electrodes

The high-resolution ultrasonic technique (impulse acoustic microscopy) was applied for observing the bulk microstructure of nanocomposites with various types of carbon nanoparticles as filler. It was shown that ultrasonic methods are excellent tools for studying nanoparticle distribution over the material bulk and for revealing probable nonuniformity. The acoustic microscopy technique allows for looking through the bulk microstructure of objects by means of layer-by-layer visualization and object cross-sectional imaging. In composites based on dispersed micrometer-sized particles of exfoliated graphite, the particle distribution over the composite material bulk was observed. In nanocomposites with various kinds of low-dimensional carbon nanofillers, i.e., nanoflakes, nanoplatelets, and nanotubes, the technique allowed the cluster architecture of the nanoparticle distribution to be revealed. Contact conjugation of low-dimensionality nanoparticles led to fractal clusters despite significant technological efforts for providing homogeneity to the nanocomposite materials and uniformity to their properties. A pronounced tendency to form micrometer-sized fractal agglomerates was found for 2D carbon nano-particles: nanoflakes and nanoplatelets. The impulse acoustic microscopy technique provides visualization of the agglomerate distribution over the nanocomposite material bulk. Another kind of nanoparticle distribution was observed with carbon nanotubes (CNTs). The latter formed CNT packings having different densities. Such regions were seen in acoustical images as small-sized areas of various brightness.

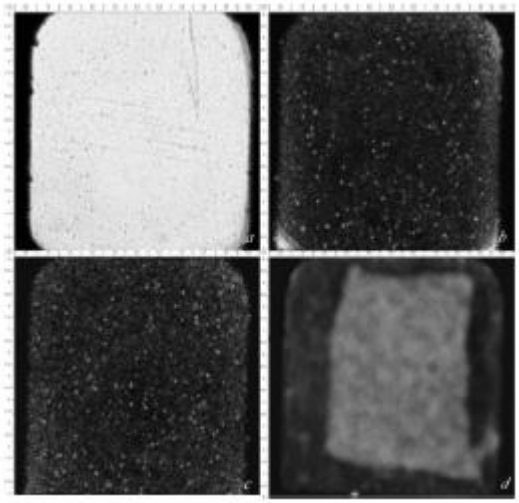

Fig. 21. Internal microstructure of carbon–epoxy nanocomposite with addition of graphite nanoplatelets (epoxy+1.0 wt.% GNP). Acoustic images (60-mm thick layers) are given at different depths inside the 1.56 mm thick specimen: (a) upper surface; (b) at 260mm deep; (c) at 380 mm deep; (d) bottom image. The dark area corresponds to the specimen fixing zone. Operation frequency is 100 MHz; scanning field is 10x11 mm2. Bright spots are agglomerates of carbon particles.

Raman characterization of nanocomposite modified screen printed electrodes

To justify the behavior of nanocomposite modifed electrodes, we characterize the nanocomposite by In-via Renishaw Raman microscope, i.e. an instrument bought with NATO funding and installed on July 2016.

We are able to study the dispersion of nanofillers on the surface of the nanocomposite using this instrument.

First of all, we acquired the Raman spectra of all filler and of pure epoxy resin, using a laser 633 nm, a grating of 600 l/mm, objective 100x and in the spectral range from 112,9 to 3480,39 (centre 2000) Raman shift/cm-1. The spectra are reported in Fig. 22 (a-d)

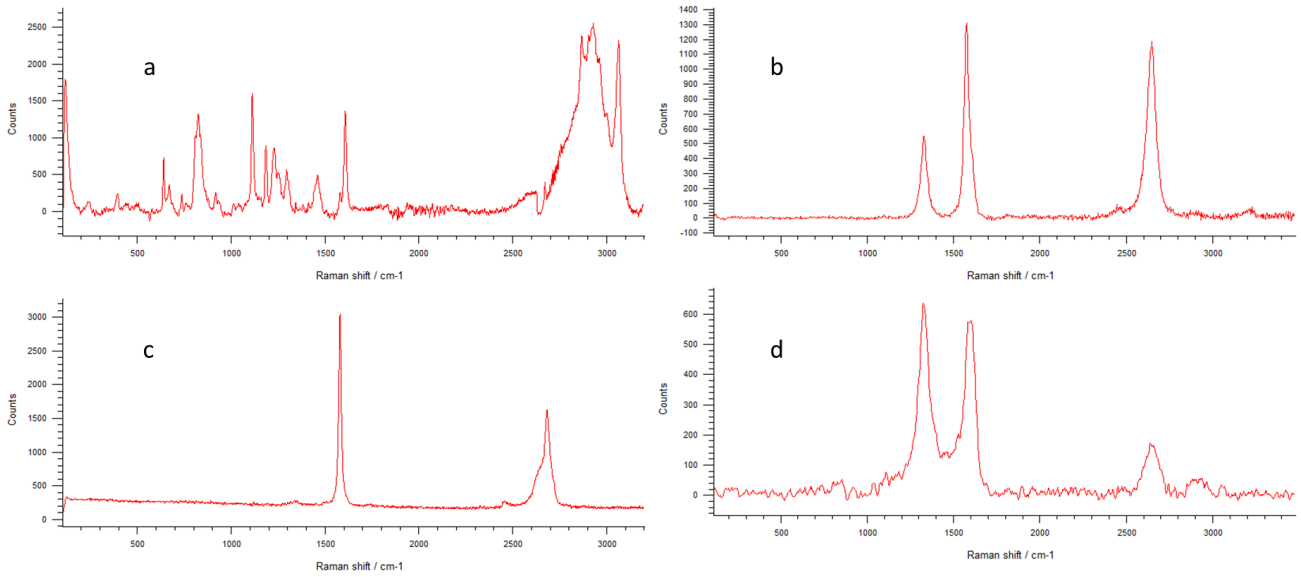

Fig. 22. Raman spectra of a) pure epoxy, b) Carbon Nanotube d=8-15 nm, C) Graphene nanoplatelets, d) Carbon Nanotube Functionalized NH2

Our aim was to observe the differences on the surface of nanocomposite modified electrodes. Therefore, we carried out a mapping measurement on the surface of nanocomposite focusing our attention on characteristic peaks of CNT (pristine and functionalized) and GNP. Unfortunately, the G band, present in CNT and GNP approximately at 1600 cm-1, is close to a signal of the pure resine. For this reason, we focused our attention at G' band, at 2700 cm-1 (Signal to Baseline from 2550.00 To 2750.00).

All mappings were performed with the following configuration: laser 633 nm, 600 l/mm grating, objective 100x and spectral range from 112,9 to 3480,39 (centre 2000) Raman shift/cm-1. The results are reported in the Fig. 23.

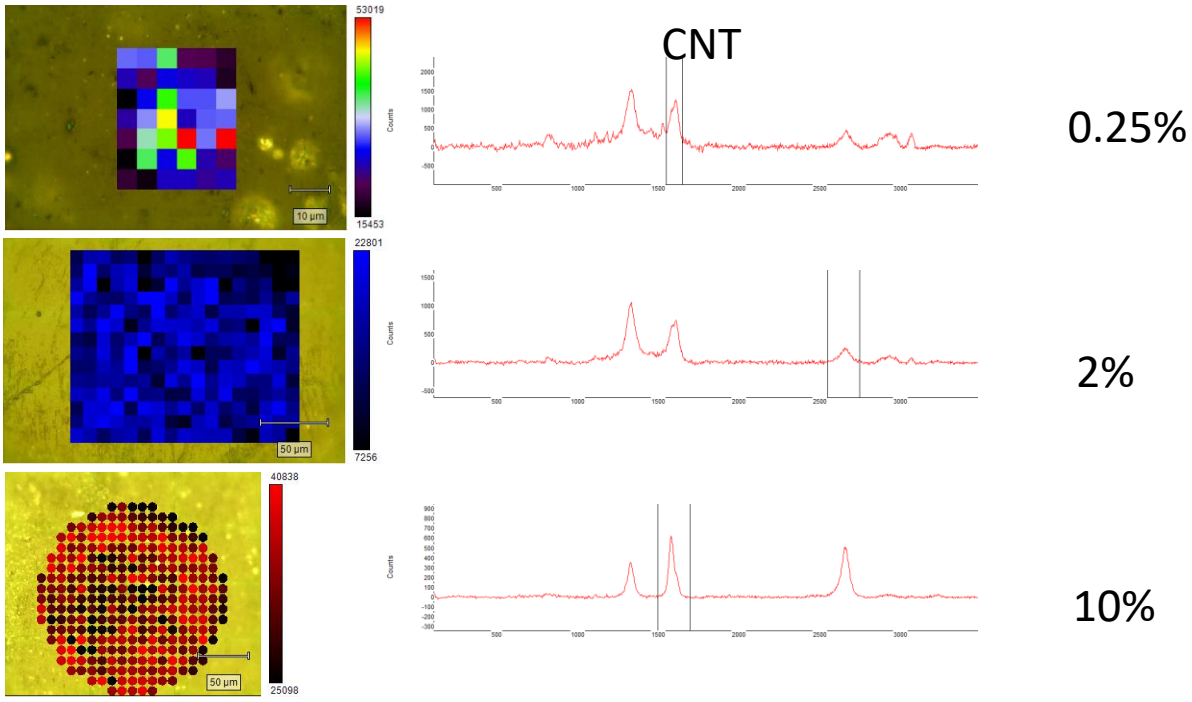

Fig. 23. Raman mapping measurements of Epoxy-CNT modified screen printed electrodes at different concentration

In all samples, we observed a change in spectrum when comparing samples loaded with 0.25% to 10% filler: in nanocomposite 0.25%, the spectrum is similar to the pure epoxy one; in nanocomposite 2%, the spectrum is the sum of pure epoxy and filler ones; in nanocomposite 10%, the spectrum is similar to pure filler.

The Raman characterization revealed that increasing the amount of fillers, they are mostly present at the surface of nanocomposite. This feature could justify the better electrochemical characteristics of nanocomposite 10% with respect to the lower concentrated ones. Furthermore, among the three nanocomposites 10% modified electrodes, CNT-NH2 and GNP modified electrodes work better than the CNT modified one. Likely, the most pronounced hydrophobic nature of pristine CNT could prevent the wettability of the nanocomposite, inhibiting charge/discharge processes, too.

III. ssDNA surface hybridization in presence of intercalating ligands

One of the important directions of DNA - chips improvement is the increasing selectivity and sensitivity in expense of enhancement of electric signal and target probe hybridization stability. Efficiency of such devices as DNA-sensors and DNA-chips depends on precise prediction of experimental parameters responsible for thermostability of nucleic acids duplexes and specific times of formation of DNA duplexes. Some following factors influence on the thermodynamics of hybridization, in particular: the density of single-strand DNA assays (the length 25-49 nucleotides) immobilized on the surface; the presence of competing hybridization; and some other factors.

Development of DNA-sensors imposes specific requirements on the effectiveness of hybridization on the interface solid-solution. One of the main requirements to the DNA-sensors is the high sensitivity and selectivity, which in its turn, demands a maximal effectiveness of hybridization and minimal non-specific adsorption on the interface of solid and liquid phases. The nucleic acids hybridization depends substantially on the temperature, salt concentration, viscosity, GC-content and other physical-chemical features. The increase of selectivity and sensitivity of DNA-sensors can be reached by using electro-chemically active compounds with higher affinity to the dsDNA than to the ssDNA. This kind of compounds can substantially increase the dsDNA stability and at the same time, the amplitude of generated signal, which increases the DNA-sensor sensitivity.

Among this kind of ligands are intercalators, molecules with flat heterocyclic structure, which fit between nucleic acids and change the local structure of dsDNA.

Below we are focused on the isotherm of hybridization of DNA on the surface in presence of ligands, binding with double - stranded regions of DNA. Let us compare the equilibrium hybridization isotherms for two idealized but experimentally accessible situations, where DNA chip immersed in solution containing intercalating ligands and: 1) only one type of single-stranded target or 2) containing targets of two different types that do not hybridize in the bulk but are both capable of hybridizing with the same probe on the surface.

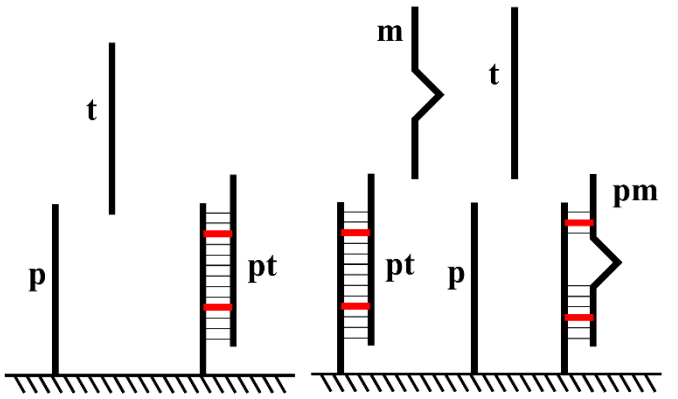

Fig. 24. The scheme of non – competing (left pane) and competing (right pane) surface hybridization affected by ligands.

The non-competitive hybridization

Let us consider the spot of N_0 single - stranded probes *p*, wherein the N_{pt} of them are hybridized with target *t*. The hybridization of *p* and *t* creates a double-stranded oligonucleotide, *pt*, at the surface. In simplest case of single species of ssDNA target, surface will be covered only by free probes *p* and hybridized ones *pt*. In this case the only reaction is

$$p + t \rightleftharpoons pt$$

and no competitive hybridization reactions occur.

$$x = \frac{N_{pt}}{N_0}$$

The dependence of the hybridization degree *x*, on the concentration of the target, c_t, is described by hybridization isotherm. For the intercalating ligands the binding reactions are written

$$\begin{aligned} pt + \ell &\rightleftharpoons pt_1 \\ pt_1 + \ell &\rightleftharpoons pt_2 \\ &\dots \\ pt_{N-1} + \ell &\rightleftharpoons pt_N, \end{aligned}$$

where *pt* is the free duplex, while pt_j is the target – probe duplex bound to *j* ligands *l* and *N* is the number of binding sites (number of nucleotides in simplified case).

In the mean field approximation the equilibrium state is defined by conditions

$$\mu_{pt} = \mu_p + \mu_t$$

$$\mu_b = \mu_\ell$$

where μ_{pt} is the chemical potential of hybridized probe *pt*, μ_t is the chemical potential of target, μ_p is the chemical potential of probe, μ_b and μ_ℓ are the chemical potentials of the bound and free ligand, correspondingly. The isotherm of hybridization is obtained in the approximation of weak solution as

$$\frac{x(1-r)^N}{c_t(1-x)} = \tilde{K}_t$$

where $\tilde{K}_t$ is the equilibrium constant, which takes into account interactions between probes and targets, including electrostatic interactions. The equilibrium distribution of ligands (ℓ) between bound and free states is described by the isotherm of adsorption

$$\frac{r}{c_\ell(1-r)} = K_\ell$$

where c_ℓ is the concentration of ligands in the bulk, *r* is the degree of ligand adsorption and K_ℓ is the equilibrium constant.

<u>The surface - competitive hybridization</u>

Let us consider the second scenario, where solvent containing targets of two different types t and m that do not hybridize in the bulk but are both capable of hybridizing with the same probe *p* on the surface. *t* is the target sequence, complementary to the probe *p*, while *m* is the mismatched sequence only partially

complementary to the probe *p*. It is supposed that the available number of binding sites for the intercalating ligands on the *pm* duplex is equal to *M* , where *M* < *N*.

If intercalation is the only mechanism of ligands binding, DNA-ligand complex formation will be restricted only by double-stranded regions. The chemical potential of the ligand bound to the complementary duplex *pt* is written

The equilibrium between ligands, targets and mismatched sequences in solution and hybridized probes is satisfied by conditions

$$\mu_b^1 = \mu_\ell$$

$$\mu_b^2 = \mu_\ell$$

$$\mu_{pt} - \mu_p = \mu_t$$

$$\mu_{pm} - \mu_p = \mu_m$$

where μ_b^1 and μ_b^2 are the chemical potentials of the ligand bound to the complementary duplex *pt* and the mismatched duplex *pm*, correspondingly. We have estimated the chemical potentials, described above in the mean – field approximation and obtained the isotherms of hybridization presented in the Fig. 25.

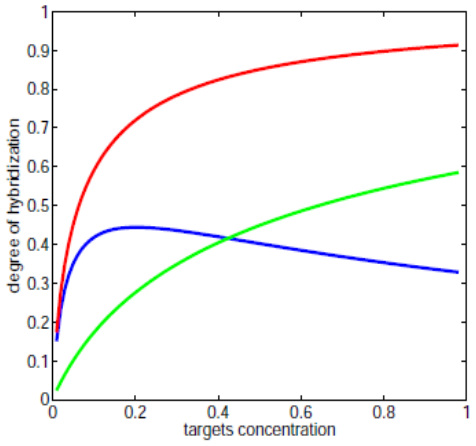

Fig. 25. Isotherm of hybridization in: ligand-free case (green line); in presence of ligands (red line). The shift of the hybridization isotherm is indicated by blue line.

Thus, intercalating ligands caused the substantially increases of the degree of hybridization.

To address the effect of ligand binding on the selectivity of DNA – chip we compare the complementary hybridization degree with the partial one and obtained that intercalating ligands substantially decrease the fraction of incorrectly hybridized probes, defined as

$$P_m = \frac{y}{y+x} ,$$

where $y = \frac{N_{pm}}{N_0}$. Behavior of the fraction of incorrectly hybridized probes in dependence on targets concentration

c_t is presented in the Fig. 26. Difference between ligand – free hybridization and those, affected by ligands is substantially defined by difference between the binding sites on the complementary and mismatched probes $\delta N = N - M$.

Thus, intercalating ligands caused the substantially increases of the selectivity of hybridization.

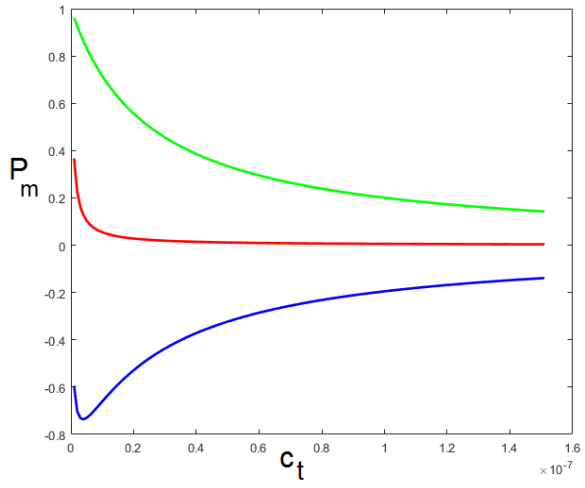

Fig. 26. The fraction of incorrectly hybridized probes in dependence on targets concentration c_t: ligand-free case (green line); in presence of ligands (red line). The shift of the incorrectly hybridized fraction δP_m is indicated by blue line. The values of parameters are:
$\ell_B \approx 7\,\dot{A}, r_D \approx 3\,\dot{A}, N = 16, M = 13, K_t = 10^9 M^{-1}, K_m = 10^{7.4} M^{-1}, K_l = 10^7 M^{-1}, c_l = 10^{-6.6} M, c_m = 10^{-6} M$
.

.

IV.Experimental work, concerning DNA biosensor prototype creation

Immobilization of ssDNA on the surface of polymer – CNT composite electrodes is a hard problem because of strong roughness of the electrode surface. Currently we are working on the problem of coating of polymer – CNT electrode by lipids molecules with subsequent immobilization of ssDNA on the lipid layer or bilayer.

To compare conductivity of lipid layer/bilayer with and without electrode surface we have measured electric features of the lipid layer/bilayer using the DNA – biosensor prototype. The principal scheme of prototype under development is presented in the Fig. 27.

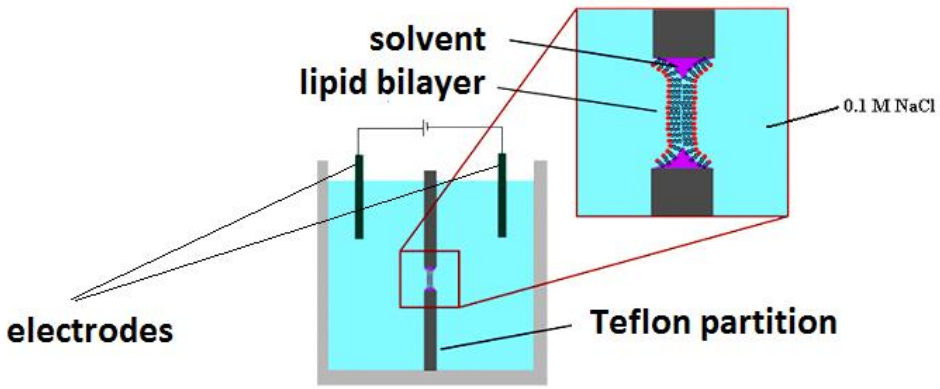

Fig.27. BLM immobilization scheme

The small amount of the lipid solution dissolved in an organic solvent is placed in the 1mm diameter hole in a Teflon wall. The wall itself is placed in the electrolyte solution (Fig.27). Before the experiment the cell initially washed up using acetone and octane and then during 10 min with the hot sulfuric acid with hydrogen peroxide.

After repeated washing with distilled water the cell was boiled in the bi-distilled water and dried. Then, we put the small amount of the lipid solution in the hole of the cell. After the solvent evaporation, the phospholipid film is formed around the hole, promoting BLM formation. Then we fill the cell with electrolyte and put it into thermostat. We used the 1,2-Dioleoyl-sn-Glycero-3-[Phospho-L-Serine] and 1,2-Diphytanoyl-sn-Glycero-3-Phosphoethanolamine, for the BLM formation.

We have used the silver chloride electrodes, placed into the cell. The potentials difference did not exceed 1mV. The cell resistance was is governed mainly by the electrolyte resistance in the hole of the cell and was about 10^3 Om, depending on the electrolyte concentration (0.1 M NaCl). The silver chloride electrodes were connected to the analog-to-digital converter (ADC, E14-140-M) and controlled with PC.

The measurement of the conductivity and capacity of BLM was conducted using the scheme, presented in the Fig.28.

Voltage is applied to membrane using ADC E14-140-M. The membrane current is also measured using ADC E14-140-M.

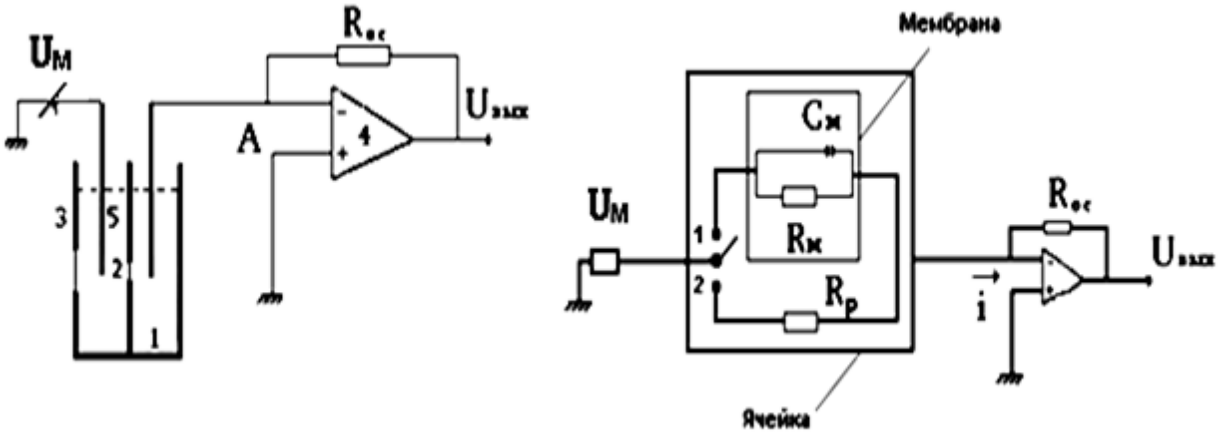

a) b)

Fig. 28. Block – scheme for the measurement of the BLM's electric parameters: a) 1 - Teflon cylinder; 2 – 1 mm hole; 3 – cuvette with electrolyte ; 4 – the operational current amplifier (Keithley 427), 5 – silver chloride electrodes, U_M - voltage applied to membrane, $U_{вых}$ – output voltage, $R_{ос}$ – the resistance of feedback loop; b)

the equivalent electric scheme: R_M – the membrane resistance, C_M – membrane electric capacity, R_p – solution resistance.

Using voltage, applied to membrane (U_M) and $U_{вых}$, and also $R_{ос}$, is possible to estimate the membrane resistance, R_M. The operational amplifier has very high input resistance. The electric current through $Rм$, mainly going through the $R_{ос}$. Then, $I_M = Uм/Rм$ and $U_{вых}/R_{ос} \approx Iм$. Consequently, the resistance of membrane is estimated as

$$\frac{\mathrm{U}м}{\mathrm{R}м} = \frac{U_{вых}}{\mathrm{R}_{ос}} \text{ or } \mathrm{R}м = \frac{Uм\mathrm{R}_{ос}}{U_{вых}}$$

and the conductivity of membrane

$$g = \frac{1}{Rм} = \frac{U_{вых}}{Uм\mathrm{R}_{ос}}$$

We also estimated the membrane resistivity as $g_{уд} = (Rм \cdot S)^{-1}$, where S is the area of the hole in the Teflon wall.

Before each experiment, we need to check the existence of the lipid membrane in the hole on the basis of the volt – ampere characteristics of BLM. We applied the triangle voltage with the amplitude $\pm U_0$ and with the scan speed α (mV/sec). The electric current consists on the resistance current I_r:

$$I_r = \frac{U}{R_M}$$

and capacity current I_c:

$$I_c = C_M \frac{dU}{dt} = C_M \alpha ,$$

where R_M is the membrane resistance, C_M is the electric capacity of membrane, and $\alpha = \frac{dU}{dt}$. For the total current through the membrane:

$$I = I_r + I_c$$

The software developed with the NI LabVIEW package is applying the saw-toothed signal on the exit of the ADC E14-140-M. The developed program is controlled the frequency and power, and read the data from ADC. It also plotted the time dependence of the applied voltage and current, etc. (Fig.29).

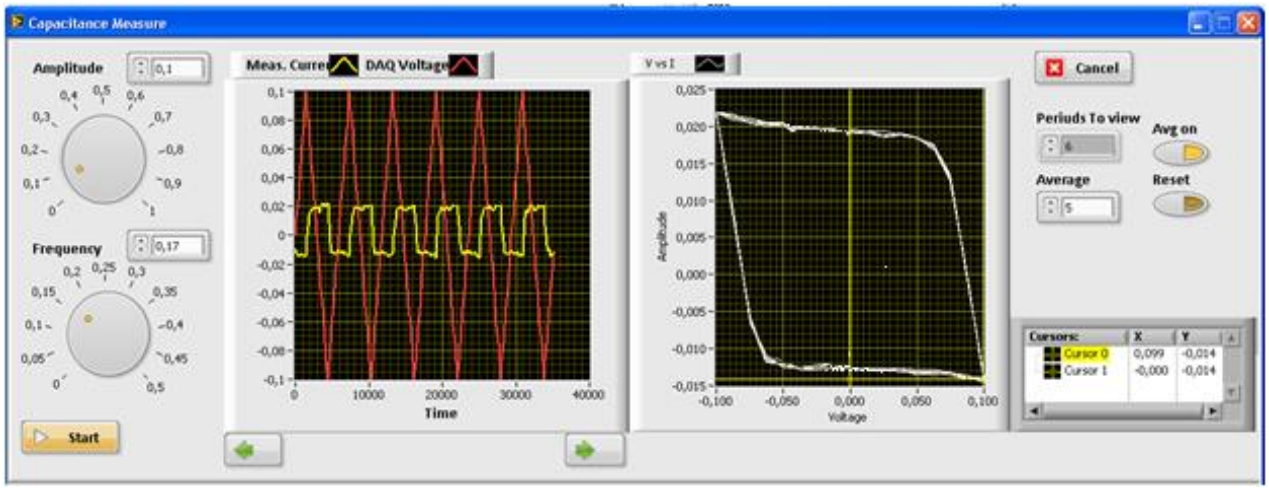

Fig. 29. The program interface for the BLM voltage – ampere cyclic characteristics.

The cyclic voltammetry is one of the most informative methods of the investigation of BLM electric features. The electric scheme, implemented for the purposes of project is presented in the Fig. 30.

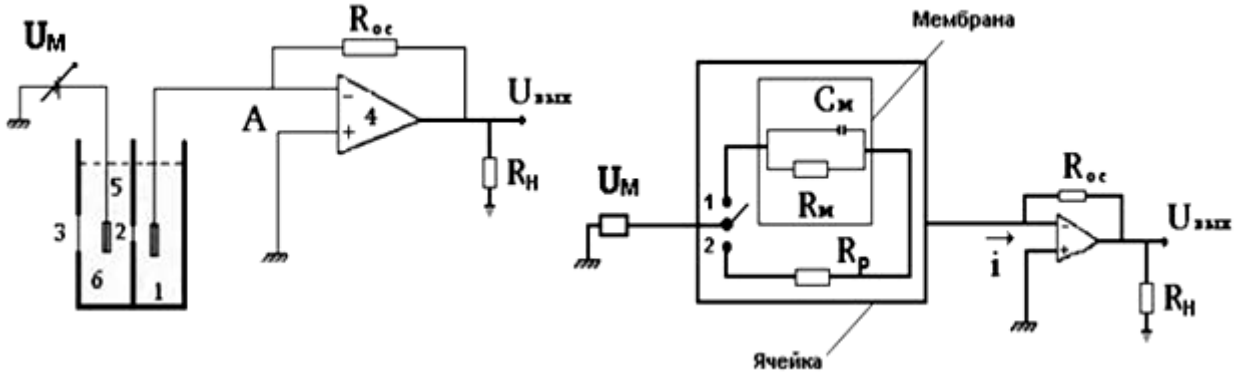

a) b)

Fig.30. The electric scheme of the BLM stability measurement in electric field: a) 1 – Teflon cylinder; 2 - hole (d = 1 mm) for the artificial mambrane; 3 – cuvette containing electrolyte; 4 - the operational current amplifier (Keithley 427) , 5 – silver chloride electrodes, U_M - voltage applied to membrane, $U_{вых}$ – output voltage, R_{oc} – the resistance of feedback loop; b) the equivalent electric scheme: R_M – the membrane resistance, C_M – membrane electric capacity, R_p – solution resistance, R_H – the load resistance.

Milestones & Deliverables

- Measurement of the stability parameter of double – stranded DNAs complexes with ligands
- The effect of intercalating ligands on the sensitivity and selectivity of the DNA - sensor
- Implementation of spin coating for preparing polymer substrate suitable for functionalization
- Raman observation of small percentage of functionalizing molecules put on the substrate
- The impulse acoustic microscopy characterization of the nanocarbon cluster architecture in the composite to modify screen printed electrodes is made
- The Raman characterization of nanocomposite modified screen printed electrodes is made
- Development of the electric scheme for the DNA – biosensor prototype

Publications by LNF Authors in the Year 2016

1. **Regulation of angiogenesis through the efficient delivery of microRNAs into endothelial cells using polyamine-coated carbon nanotubes,** Andrea Masotti, Mark R Miller, Antonella Celluzzi, Lorraine Rose, Federico Micciulla, Patrick WF Hadoke, Stefano Bellucci, Andrea Caporali, Nanomedicine:Nanotechnology, Biology and Medicine, Published Online: March 21, 2016, DOI: http://dx.doi.org/10.1016/j.nano.2016.02.017.

2. **Biological interactions of carbon-based nanomaterials: From coronation to degradation**, K Bhattacharya, SP Mukherjee, A Gallud, SC Burkert, S Bistarelli, S. Bellucci, M. Bottini, A. Star, B. Fadeel, Nanomedicine: Nanotechnology, Biology and Medicine, Volume **12**, Issue 2, February 2016, Pages 333–351

List of Conference Talks by LNF Authors in the Year 2016

S. Bellucci, Nanomaterials in Bio-Engineering: what are they, where can they be found ?, UNIVPM Seminar, Ancona, May 13, 2016